

Gravity inversion of deep-crust and mantle interfaces in the Three Gorges area

Wang Jian^{1,2}, Shen Chongyang^{1,2}, Li Hui^{1,2}, Sun Shaoan^{1,2} and Xing Lelin^{1,2}

¹Key laboratory of Earthquake Geodesy, Institute of seismology, China Earthquake Administration, Wuhan 430071, China

²Crustal Movement Laboratory, Wuhan 430071, China

Abstract: To better understand the heterogeneity of deep-crust and mantle interfaces in the region of the Three Gorges, China, we used the Parker-Oldenburg iterative inversion method to invert existing Bouguer gravity data from the Three Gorges area (1 : 500000), a new gravity map of the Three Gorges Dam (1 : 200000), and the results of deep seismic soundings. The inversion results show a Moho depth of 42 km between Badong and Zigui and the depth of the B2 lower-crustal interface beneath the Jiangnan Plain and surrounding areas at 21–25 km. The morphology of crustal interfaces and the surface geology present an overpass structure. The mid-crust beneath the Three Gorges Dam is approximately 9 km thick, which is the thinnest in the Three Gorges area and may be related to the shallow low-density body near the Huangling anticline. The upper crust is seismogenic, and there is a close relationship between seismicity and the deep-crust and mantle interfaces. For example, the M5.1 Zigui earthquake occurred where the gradients of the Moho and the B2 interface are the steepest, showing that deep structure has a very important effect on regional seismicity.

Key words: inversion; gravity anomaly; deep structure; the Three Gorges area

1 Introduction

The inversion of gravity data to study deep-crust and mantle interfaces has implications for understanding regional geology and seismicity. It provides higher lateral resolution than other geophysical methods. Furthermore, it is suitable for regional studies and can be used with other types of data in joint inversions.

The Three Gorges region is the site of a large water control project in China, and its crustal structure and

stability are well studied. Wang^[1] studied the crustal structure of the area by using 1 : 500000 Bouguer gravity data and artificial sounding data. This paper utilizes the same dataset as well as a new Bouguer gravity dataset (1 : 200000) and recent results of deep seismic sounding data. We also explore the relationship between deep crustal and mantle structure and regional seismicity.

To obtain a new image of deep-crustal and mantle interfaces in the Three Gorges area, we adopt the Parker-Oldenburg iterative inversion method^[1,2] and use a spliced map of Bouguer gravity data (1 : 500000, 1 : 200000) and deep seismic sounding data. We also analyze and discuss the inversion results with respect to regional tectonics and seismicity.

Received:2012-06-07; Accepted:2012-08-02

Corresponding author:Shen Chongyang, E-mail:scy907@163.com

Author: Wang Jian, major in gravity field change and lithosphere structure; E-mail:wangjian447@yahoo.com.cn

This work is supported by grant 201008001 from China Earthquake Administration, 201156085 from Institute of Seismology, China Earthquake Administration.

2 Principle of the inversion method

2.1 Basic principle of the Parker-Oldenburg iterative inversion

The Parker equation^[3] can be used for the forward calculation of gravity:

$$F[\Delta g(\hat{r}_0)] = -2\pi G e^{kz_0} \sum_{n=1}^{\infty} \frac{k^{n-1}}{n!} F[\rho(r) \cdot h^n(r)] \quad (1)$$

where $F[\]$ is the Fourier transform, ρ is the two-dimensional density distribution, and k is the wave number.

Using a series expansion of equation (1), we can obtain its iterative form^[4]:

$$F[h(\hat{r})] = -\frac{F[\Delta g]}{2\pi G \rho} e^{kz_0} - \sum_{n=2}^{\infty} \frac{k^{n-1}}{n!} F[h^n(r)] \quad (2)$$

Instead of computing the Fourier transform in equation (1), equation (2) can use the FFT algorithm, which quickly converges and is more stable for large model spaces.

The inversion is completed in two iterative processes: in the first cycle, the interface of the lower layer is successively translated, and the gravity resulting from the new model is calculated; in the second cycle, the perturbation to the upper interface (Δh) is calculated, instead of directly calculating h using equation (2). The perturbation to the lower interface can be obtained using the average perturbation to the upper interface. If Δg_{cal}^m is a gravity anomaly in model m , then the difference between the forward-modeled gravity anomaly and the observed gravity anomaly is the model's correction:

$$\Delta g_{\text{inv}}^m = [\Delta g_{\text{inv}}^{(m-1)} + (\Delta g_{\text{obs}} - \Delta g_{\text{cal}}^m)]/2 \quad (3)$$

where m represents the number of the iteration.

2.2 Regularization

Due to the downward continuation factor e_0^{-kz} , the impact

of high-frequency components of the gravity data is greatly enhanced. To enhance the stability of the inversion, we introduce a regularization parameter to equation (2):

$$\nu(\alpha) = 1 / (1 + \alpha e^{2|k|z_0}) \quad (4)$$

and equation (2) becomes

$$F[h(r)] = -\frac{F[\Delta g]}{2\pi G \rho} \frac{e^{kz_0}}{(1 + \alpha e^{2|k|z_0})} - \sum_{n=2}^{\infty} \frac{k^{n-1}}{n!} F[h^n(r)] \quad (5)$$

We can make the inversion results more consistent with the results of deep seismic soundings by adjusting the regularization parameter.

2.3 Weighted alternating iterative approach

Using equation (5), the iterative inverse correction is

$$F[\Delta(\rho h(r))] = -\xi \frac{F[\Delta g_{\text{inv}}]}{2\pi G} \frac{e^{kz_0}}{(1 + \alpha e^{2|k|z_0})} \quad (6)$$

Let $\rho h = w$. Then,

$$\Delta w = h\Delta\rho + \rho\Delta h \quad (7)$$

Density and interface depth have different implications for the gravity potential field. It is typically difficult to distinguish them in gravity inversion; the effects of density and interface depth on gravity are mainly high-frequency and second-order effects. The high-frequency effect of density is up to one half smaller than that for interface depth, but the two effects are equal in their low-frequency components^[2].

In this paper, we use a weighted alternating iterative method to deal with this ambiguity. In the first iteration, the correction to the interface depth (Δh) is calculated; in the second iteration, a new gravity model ($(g(h_i, \rho_{\text{new}}))$) is calculated based on the interface depth corrections by using equation (3). We calculate the model's range correction and Δw to correct the density in this iteration ($\Delta\rho$). This process is repeated until certain accuracy requirements are met, as shown in figure 1.

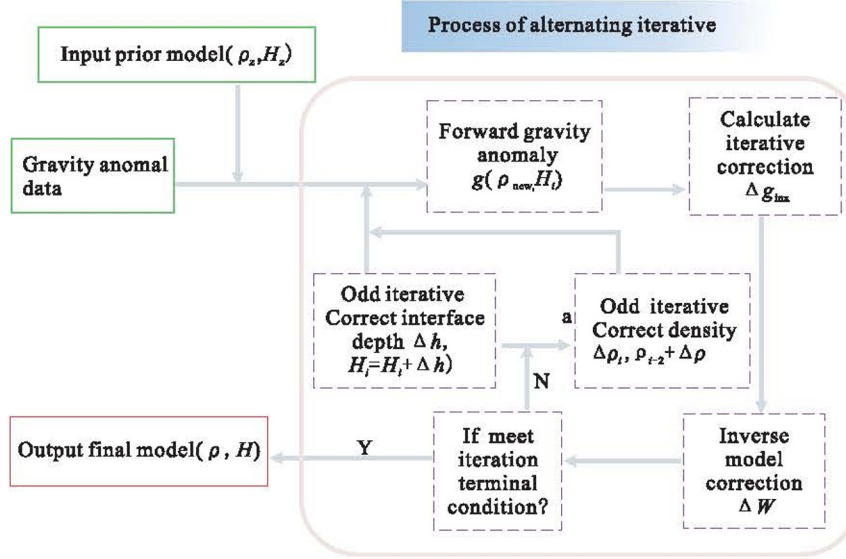


Figure 1 The process of the weighted alternating iterative inversion

2.4 Multi-layer density interface inversion

The inversion of multi-layer density interfaces is based on a single density interface inversion. The isolation of gravity anomalies is the key problem in transitioning from the inversion of a single layer to the inversion of multiple density interfaces^[5]. There are many methods of separating gravity anomalies, including the mean field method, the cutting method, and wavelet analysis^[6].

We use the peeling method (layer-by-layer inversion from bottom to top) and successively calculate the main crustal interfaces. First, an average layered model is established, including the reference depth of each layer and the density difference between each layer. The inversion process begins from the Moho, where the inversion results are mostly consistent with the deep seismic sounding results. The gravity anomaly associated with the Moho is calculated, and the upper interface is inverted. This process is repeated for all crustal interfaces^[7].

3 Data processing

3.1 Data

The data consist of two parts: gravity data and constraint data. The gravity data are from the Hubei Geological Survey Institute, and they include a map of the

Three Gorges area (29° 20′ – 32° 20′ N, 109° 30′ – 112° 3′ E), Bouguer gravity data (1 : 500000) and a gravity map of the Three Gorges Dam (30° 40′ – 31° 20′ N, 110° – 112° E; 1 : 200000). The constraint data include seismic sounding^[8,9] and tomography results^[10,11]. Because seismic soundings and tomography have higher accuracies than gravity inversion results, we use these results as constraints. The locations of the seismic sounding and tomography profiles are shown in figure 3. Adding constraints to the inversion can greatly improve the non-uniqueness of the problem; we make use of prior information to determine interface depths at selected locations using these known depths as constraints. We use the average velocity of the existing layered crustal model^[1] (Fig. 2).

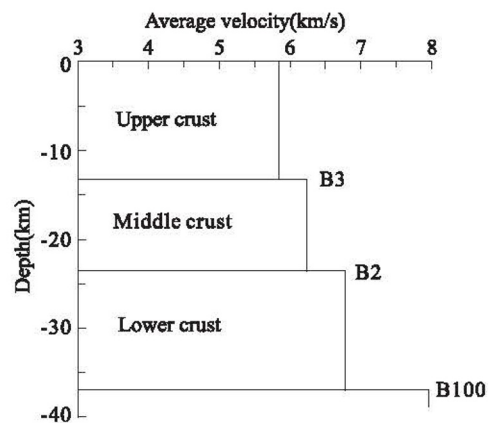
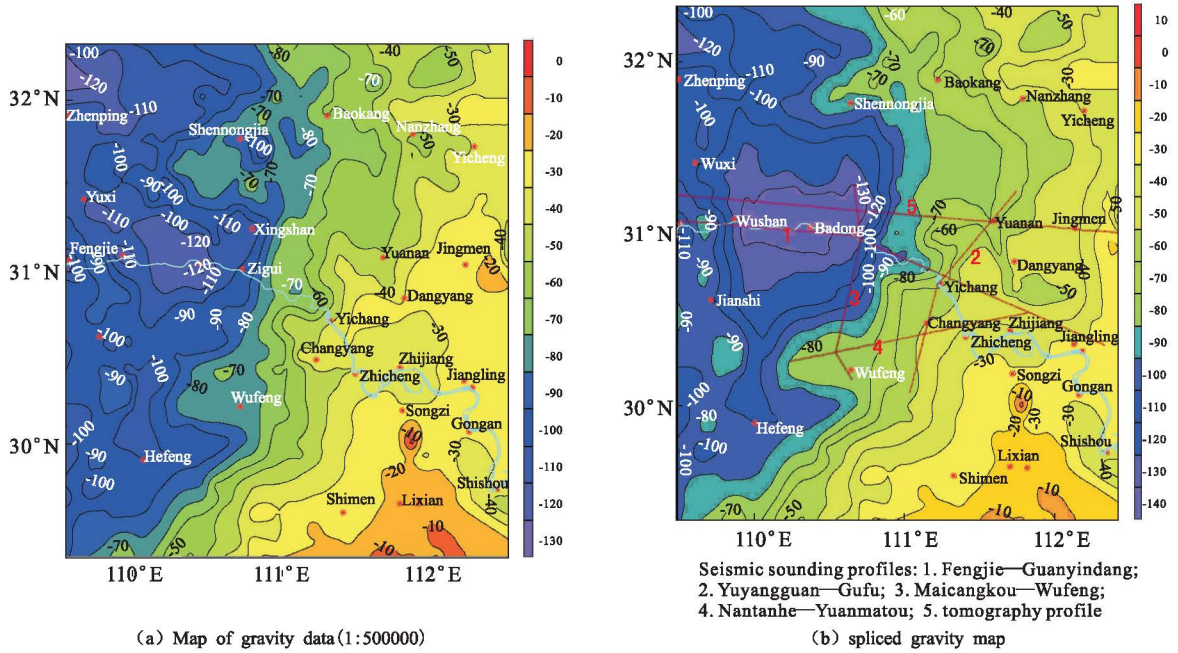


Figure 2 Model of crustal layering in the Three Gorges area



(a) Map of gravity data(1:500000)

(b) spliced gravity map

Figure 3 Map of gravity data and the locations of deep soundings in the Three Gorges area

We convert P-wave velocity (V) into medium density (ρ) according to the empirical equation between V and ρ ^[1]. The average depth of each interface can be selected from figure 2.

$$\begin{cases} \rho = 2.78 + 0.27(\nu - 6.0), \nu < 5.5 \\ \rho = 2.78 + 0.56(\nu - 6.0), 5.5 \leq \nu \leq 6.0 \\ \rho = 3.07 + 0.29(\nu - 7.0), 6.0 \leq \nu \leq 7.5 \\ \rho = 3.07 + 0.29(\nu - 7.0), 7.5 \leq \nu \leq 8.5 \end{cases} \quad (8)$$

3.2 Data processing

To suppress boundary effects, we use the symmetry extension and interpolation extension methods to extend the raw data to form a larger regional background model for the inversion. Within the Three Gorges area, the splicing of different-resolution Bouguer gravity maps (1 : 500000 and 1 : 200000) is problematic. Outside of the Three Gorges area, we must use symmetry extension and interpolation extension to suppress boundary effects due to the lack of gravity data.

To splice Bouguer gravity maps of different resolutions, we grid the two maps at a scale of $1.43' \times 1.43'$, and the value of each grid point is obtained by interpolation. In the Three Gorges area, we use the higher-resolution Bouguer gravity data (1 : 200000); outside of the Three Gorges Dam area,

10-column data is linearly interpolated, instead of the 1 : 500000 Bouguer gravity data in the corresponding area. In the other area, we use the 1 : 500000 Bouguer gravity data, which results in a reasonable splicing map (Fig. 3 (b)). A comparison to the map of the 1 : 500000 gravity data (Fig. 3 (a)) shows that the maps are spliced very well and that there are no large jumps in data. The spliced map and the original map show the same morphological characteristics, including deep and shallow crustal gravity anomalies. We extend the spliced gravity data from $3^\circ \times 3^\circ$ to $6^\circ \times 6^\circ$, which is used for the actual inversion.

4 Results

4.1 Convergence and accuracy of the inversion

We invert for upper, middle, and lower crustal interfaces (B3, B2, and B1) in the Three Gorges area. We set the maximum number of iterations to 15, and the convergence is shown in figure 4 (the vertical axis represents the mean square error of the adjacent iterative inversion).

Figure 4 demonstrates the rapid convergence of each interface. The rate of convergence decreases as the inversion depth decreases. The choice of regularization

parameters depends on the conformity between the inversion and seismic sounding results. Due to the differing resolutions caused by their methods of calculation, these results do not completely agree. The inversion continues until the root mean square (RMS) between the inversion results and the seismic soundings is less than 2.0 km, limiting the accuracy of the inversion results. Figure 5 shows a comparison of the inversion results and the seismic sounding results for the Fengjie-Guanyindang profile, with RMS of the B1, B2, and B3 interfaces of 1.3 km, 1.578 km, and 1.807 km, respectively.

Figure 6 shows the forward-modeled gravity anomalies for the inverted interface model. There is a strong similarity between interface depth and gravity, calculated using equation (1); the morphological characteristics are consistent between the models. Superimposing the gravity anomaly associated with each interface shows that the total forward-modeled gravity anomaly agrees with the hierarchical model, which indicates that the inversion results are accurate and reliable.

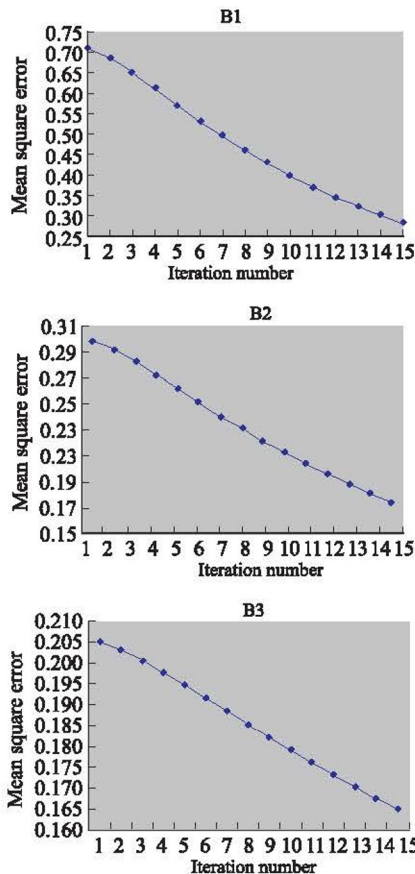


Figure 4 Convergence curves of the inversion

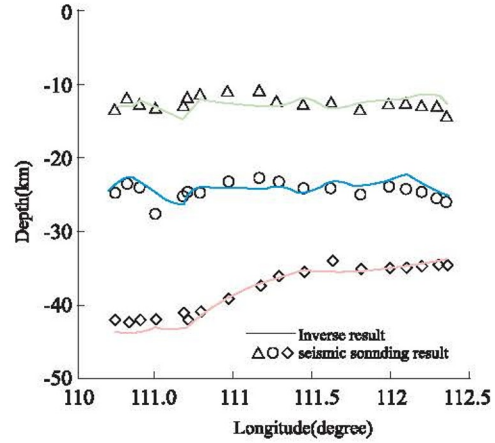


Figure 5 Comparison of the inverted crustal interfaces using the potential field data with the deep sounding results along the Fengjie-Guanyindang profile

4.2 The B1 interface

The depth of the B1 interface (Moho) reflects the crustal thickness. Figure 7(a) shows that the depth of the B1 interface increases from 33 km in the east of the study area to 43 km in the west, which is consistent with the deep seismic sounding results^[10]. The general morphology of the Moho shows medium-wavelength undulations, with subsidiary short-wavelength variations. Near 111° E, there is a NNE-trend in Moho depth, which corresponds to the location of the eastern China gradient belt. East of this belt, the Moho of the Jiangnan-Dongting Basin smoothly fluctuates from 33 to 36 km depth, while the Moho beneath the western Hubei mountainous region to the west varies between 38 and 43 km. There are many fluctuations in the Moho that form relative areas of crustal thinning and thickening, such as the Moho uplift near Shishou-Gongan (Moho depth of approximately 34 km), the Moho depression near Badong-Zigui (Moho deeper than 40 km), and the Moho uplift near Shennongjia (Moho shallower than 39 km). The Shennongjia area is situated in the highest terrain of the Three Gorges area, with a peak altitude above 3000 m. If this area is locally gravitationally compensated, the Moho depth should be deepest in this area; however, it is shallower than beneath Badong (highest altitude of 2000 m), which shows that this area is not in equilibrium. South of 111° E, the Moho depths change more rapidly than north of 111° E. The depth contours trend more NNE

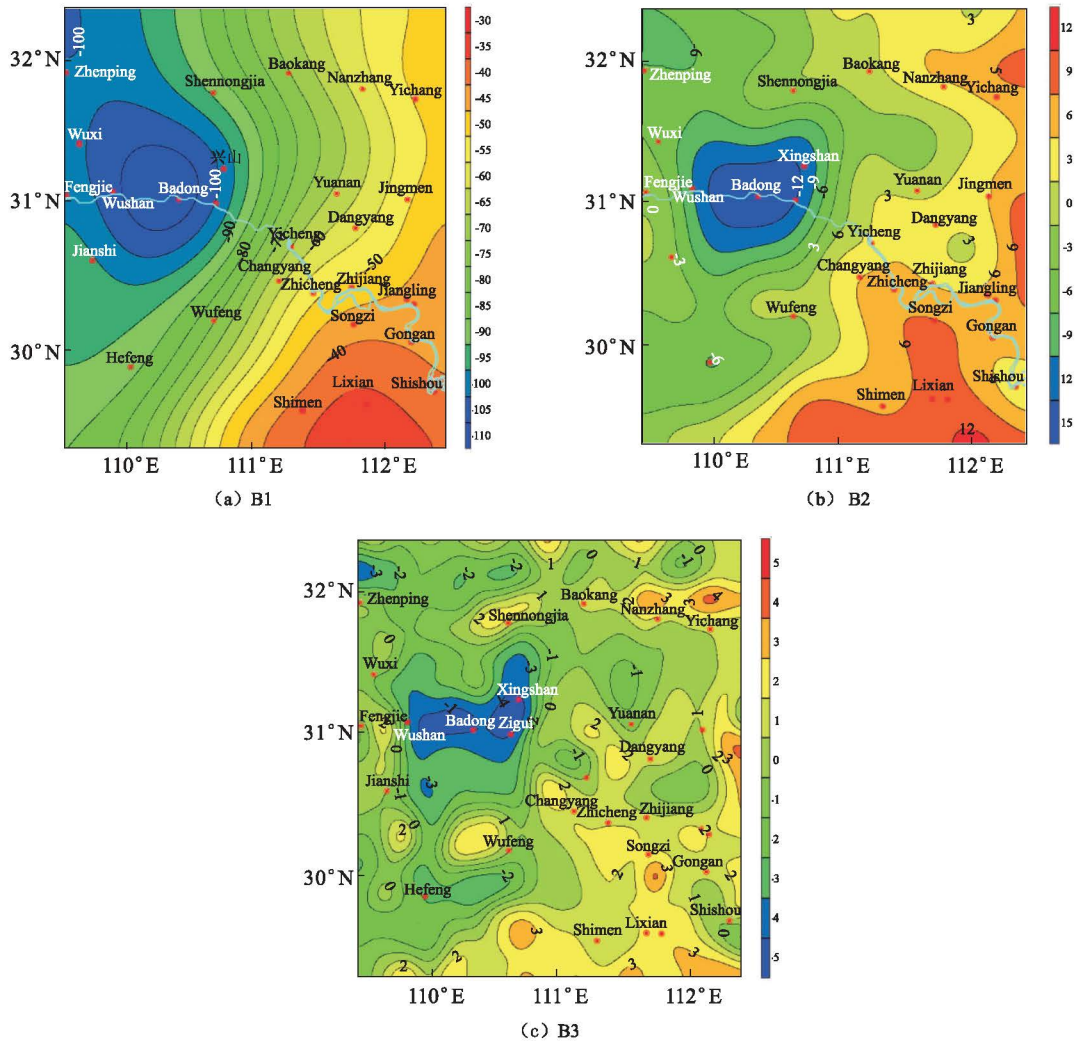


Figure 6 Forward-modeled gravity anomalies of the B1, B2, and B3 interfaces (mGal).

in the Zhenping-Baokang area, while they trend NE in the Nanzhang-Yicheng area.

4.3 The B2 interface

The B2 interface represents the bottom surface of the mid-crust. As shown in figure 7(b), the B2 interface changes smoothly, with many local minima and maxima. The depth of B2 ranges from 21 km to 28 km, which is very similar to the deep seismic sounding results^[10]. Its general morphology is consistent with prior inversion results^[11]. The depth of the B2 interface shallows to the east and deepens to the west. Near 111°E, the depth contours have a nearly N-S trend, and the B2 interface is generally flat (between 24 and 26 km). East of 111°E, the interface fluctuates relatively smoothly, while it fluctuates more to the west. Along 32°N, the depth contours have a nearly E-W trend, with the depth of the B2 interface increas-

ing from north (23 km) to south (25 km), which reflects that there may be an E-W-trending zone of variation. The Baokang-Yuanan lies in a NNW-trending depression (23 – 25 km), as do the Zigui Basin and Hefeng.

4.4 The B3 interface

The B3 interface represents the bottom surface of the upper crust. As is shown in figure 7(c), the depth of the B3 interface ranges from 8 to 16 km. Along 111°E, the depth contours have a nearly N-S trend, with smoother changes to the east than to the west. To the west, the interface depth varies rapidly, with a series of short-wavelength undulations; the Zhenping-Fangxian-Xiangfan area to the north lies in an E-W-trending depression. Compared to the B2 interface, the NNW trend in Baokang-Yuanan is more obvious. The B3 interface is shallower east and west of Yichang, but

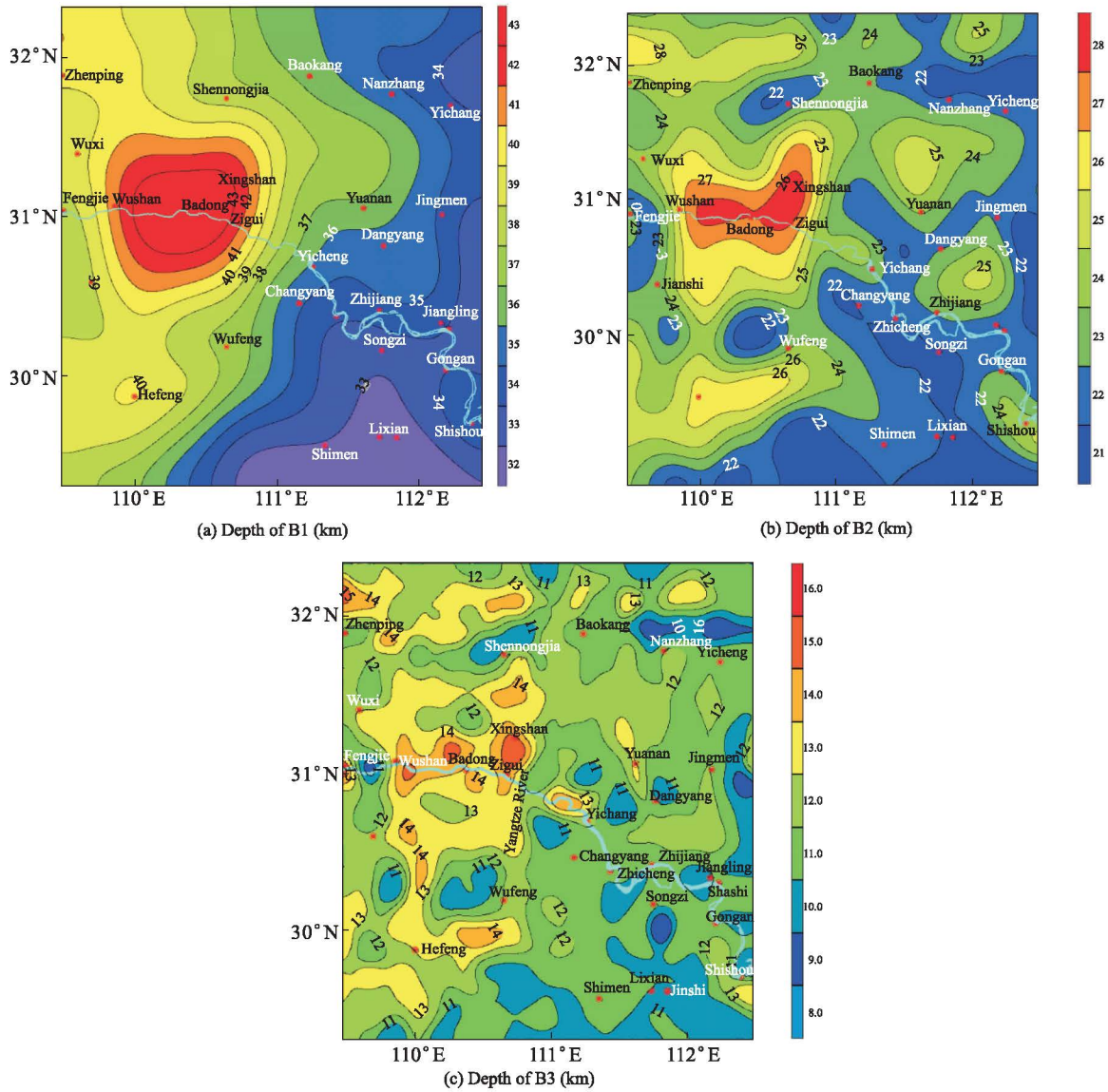


Figure 7 Isobathic map of the B1, B2, and B3 interfaces in the Three Gorges area

it is deeper than 13 km north of Yichang. The Wangdi-an-Yidu area lies in a local depression at 12 – 13 km depth, revealing the structure of the western Jiangnan Basin. There is an area of local uplift north of Shennongjia where the B3 interface is shallower than 14 km.

Integrating the undulations in the B1, B2, and B3 interfaces in the Three Gorges area shows that the upper crust is slightly shallower to the east (12 km depth) and deeper to the west (13 km depth). In Badong-Zigui, the B3 interface reaches a depth of 15 km. The average thickness of the mid-crust is 12 km, with perturbations that are generally small. The thinnest area is in Sandouping, where the mid-crust is only 9 km thick. The variations in the thickness of the lower

crust are large, with an average thickness of 10 km to the east and 15 km to the west. The thickness of the crust is most affected by the lower crust, followed by the upper crust.

5 Relationship between earthquakes and deep structure

The main structure of the Three Gorges area contains developing faults, including the Hubei tectonic belt in the northwest, the Hubei fold belt to the southwest and the central Hubei block. The earthquakes in this area are mainly distributed in the Hubei tectonic belt and the central Hubei block. The Hubei tectonic belt trends NWW, which corresponds to the E-W-trending

depth variations at 32°N . The Hubei fold belt is composed of a series of compound folds (NW to NNW), consistent with contours of the B2 interface. The undulation of the B3 interface may be related to the formation of compound folds and faults. The strike of the fault in the central Hubei block is NW to NNW, consistent with the depth of the B2 interface. Here, the B3 interface has a close relationship with larger structures and deeper interfaces.

Figure 8(a) shows an E-W-trending vertical profile at 31°N in the Three Gorges area that crosses the Huangling anticline, the Zigui Basin, the Dangyang Basin, and several major tectonic areas, revealing the structure of deep interfaces. The Moho is deepest in Fengjie-Zuigui, where it forms a local depression to 43

km depth. The depth of the Moho gradually decreases from Zigui to the east. The B2 interface has medium-wavelength undulations, and there is a local depression of the interface to a depth of 27 km in Zigui-Badong and to a depth of 23–24 km east of Zigui. The B3 interface also has a local depression in Zigui-Badong, and it undulates between 10 and 15 km depth to the east with a medium wavelength. Most of the seismicity occurs in the Zigui-Badong area, where the B3 interface has small undulations and an average depth of 14 km. In the Yuanan fault zone, the depth of the B3 interface decreases and there is relatively abundant seismotectonic activity, which shows that the mid-crust in this area is unstable.

Figure 8(b) shows a vertical N-S profile at 111°E

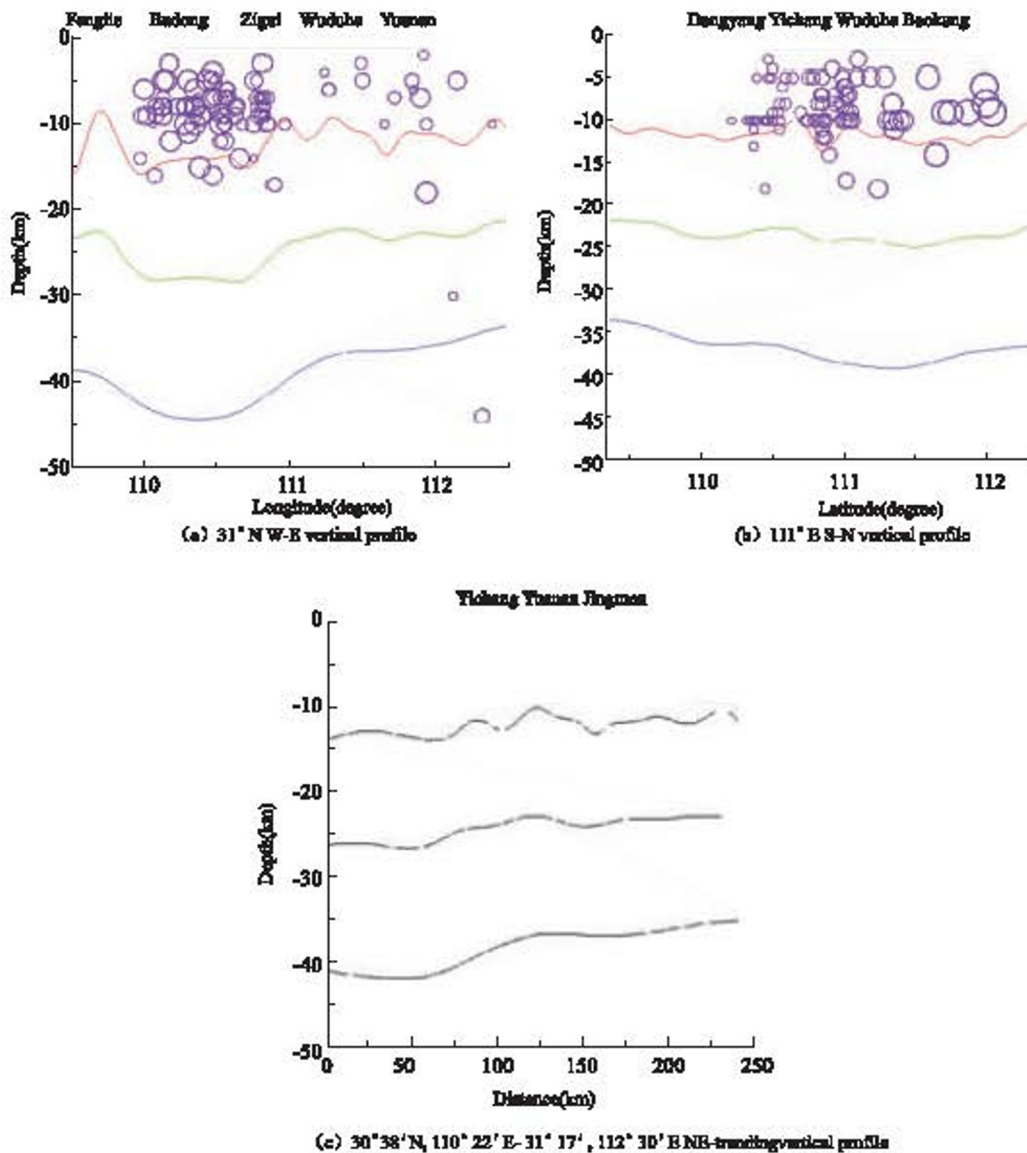


Figure 8 Vertical profiles of the Three Gorges area

that crosses the core of the Huangling anticline and reveals its deep structure. The B1 and B2 interfaces change smoothly and their depths increase by up to 4 km from south to north. The B2 interface changes more gently than the B1 interface. In Changyang-Wuduhe, the depth of the B3 interface clearly changes, and Sandouping (the Three Gorges dam site) lies in a local depression of the B3 interface where it is at its maximum depth of 13 km.

Figure 8(c) shows a vertical profile at (30° 38' N, 110°22' E) to (31° 17' N, 112° 30' E) of NE that crosses the Huangling anticline, the Yuanan fault zone, the Wuduhe fault zone, and several major tectonic areas. Figure 9(c) shows that the B1, B2, and B3 interfaces undulate unevenly, although the depths of the B1 and B2 interfaces change relatively gently. Similar to figure 9(a), the interface depths increase from east to west and each interface is at its deepest in the Zigui Basin. The B3 interface shows some small local variations, with a about 1 km greater depth in Dangyang than in surrounding areas. There is some local uplift in Yichang and Yuanan, where the B3 interface is at its maximum depth in this profile (10 km).

These three profiles are representative of the Three Gorges area. They cross several major tectonic areas and reveal the structure of deep interfaces.

Figure 9 shows the distribution of $M_s \geq 3.0$ seismicity from 1960 to 2010 in the Three Gorges area. Seismicity mainly occurs in NNW and NNE trends aligned with a series of faults in the Huangling anticline and the surrounding area, at depths of 5 – 15 km in the upper and mid-crust. These faults are basal faults, have limited extents, and are controlled by NW-NNW structure. Previous studies of earthquake geology, crustal deformation, and focal mechanisms show that modern structural activity in this area is mainly influenced by the extensional stress field, as evidenced by extensional fault activity^[12]. Therefore, earthquakes in this area occur infrequently and with low intensities.

Figures 8(a) and (b) show the distributions of $M_s \geq 3.0$ seismicity from 1980 to 2010 along 31° N and 111° E, respectively, with profile widths of 20 km. Most of the small- and medium-sized earthquakes occurred in the upper crust at 5 – 15 km depth, with $M_s \geq 4.0$ earthquakes mainly between 12 and 16 km depth.

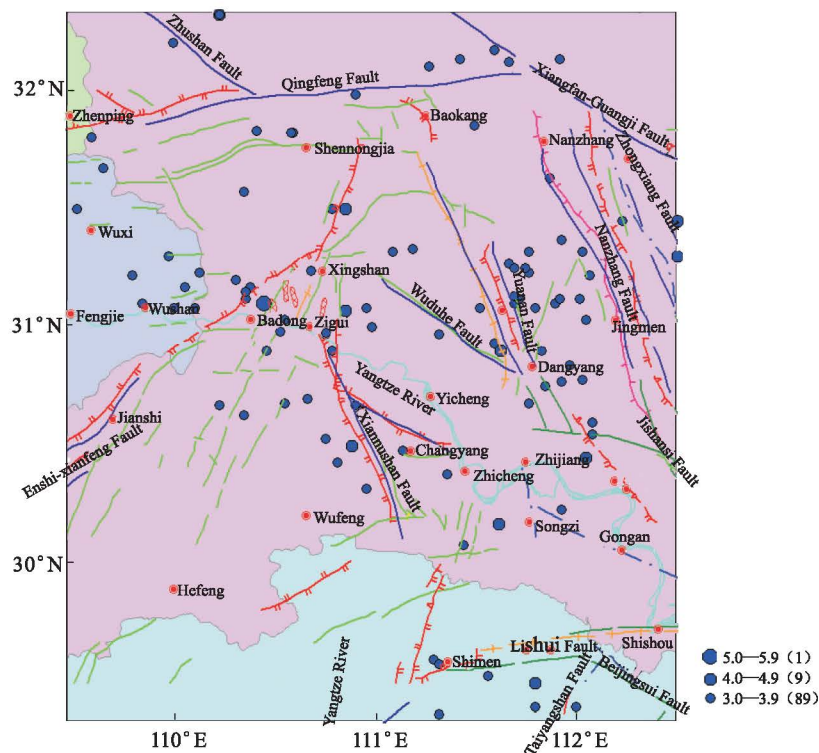


Figure 9 Distribution of seismicity in the Three Gorges area

The Zigui Longhuiguan earthquake ($M_s 5.1$) is the largest earthquake recorded in the Three Gorges area. It occurred along a series of NE-trending faults^[13]. With respect to the gravity field, the seismogenic zone lies west of the eastern China gradient belt and in the area of the largest changes in crustal interfaces. In this area, the Moho is at a depth of 43 km, and the B2 interface is at a depth of 28 km. The seismogenic zone is located in a zone where interface depths change from shallow to deep. In the seismogenic zone, the depth of the B3 interface is 14 km and at the edge of a 14 – 16 km local depression. The NE trend of the 14 km isoline of the B3 interface is consistent with the seismogenic zone, which shows that the NE-trending fault zone may have developed to the bottom of the upper crust and is confirmed by the 16 km source depth of the Zigui earthquake.

Comparing the distribution of earthquakes with the interfaces shows that most of the large earthquakes occur in a zone of transition from uplift to depression. These areas have sharp interface gradients and usually have larger faults at the surface, demonstrating the close relationship between the undulation of the deep interfaces and seismicity.

6 Conclusions

The main characteristics of the inversion results are consistent with those of Wang^[1], although there are some differences near the Three Gorges Dam; the depth of the Moho in Zigui-Badong increases from 39 km in Wang's model to 42 km in our model; the depth range of the B2 interface increases from 24 – 27 km to 21 – 28 km; and our results are more similar to deep seismic sounding results that show that the B2 interface is at depth between 21 and 29 km^[10], mainly in the Jiangnan Basin and the surrounding area. The undulation of the B3 interface in the Three Gorges Dam area is more precise, showing several areas of local uplift around the Three Gorges Dam. These differences may be due to the joint inversion of higher-resolution gravity data (1 : 200000), which improves the spectral resolution for the Three Gorges area and improves the resolution of interfaces in the Three Gorges area, particularly near the dam. The inclusion of more spectral in-

formation also impacts the regularization parameter, causing high-frequency components of the gravity data to be filtered differently and affecting the inversion results for the entire area.

In the Sandouping area (the Three Gorges dam), the B1 interface is at a depth of 37 km and lies in a NNE-trending zone of varying interface depths. The depths of the B2 and B3 interfaces in this area are deeper than in surrounding areas, and the mid-crust is thinnest here (9 km) out of the larger Three Gorges area (about 12 km). The upper crust in the Sandouping area is 13 km thick, which is approximately 2 km thicker than in surrounding areas, which may be related to the large low-density region in the middle of the Huangling anticline. The low-density region and the surrounding rock increase the thickness of the upper crust, resulting in a thinner mid-crust.

Comparing the general morphology of the deep-crust and mantle interfaces with surface geology shows an arch between them, particularly in the northwestern Hubei area. In this area, a NNE-trending mantle uplift belt and the nearly E-W-trending Qinling Indo-China orogenic belt intersect at a high angle, which decreases from north to south.

There is a close relationship between seismicity and interface morphology. Earthquakes mainly occur along a NNW trend (Yuanan Graben Fault, Xiannüshan Fault) and a NNE trend (Xinhua Fault, Niukou Fault) around the Huangling anticline. Earthquakes usually occur in the upper crust and are mainly small-to-moderate in size ($2 < M_s < 4$). Many relatively large earthquakes occur in the area between uplift and depression, where active faults are located.

References

- [1] Wang Shiren, Zhu Silin and Li Rongchuan. Three dimensional inversion of gravity anomalies in the region of three gorges, the Yangtze River. Chinese Journal Geophysics, 1992, 35(1) : 69 – 76. (in Chinese)
- [2] Feng Rui, Yan Huifen and Zhang Ruoshui. A computation method of potential field with three-dimensional density and magnetization distributions. Acta Geophysica Sinica, 1986, 29(4) : 399 – 406. (in Chinese)
- [3] Parker R L. The rapid calculation of potential anomalies. Geophys, 1972, 31(1) : 447 – 455.
- [4] Oldenburg D W. The inversion and interpretation of gravity anom-

- alies. *Geophysics*, 1974, 39(4):526–536.
- [5] Guo Lianghai and Meng Xiaohong. The correlation method for gravity anomaly separation. *Progress in geophysics*, 2008, 23(5):1425-1430. (in Chinese)
- [6] Yang Wencai, Shi Zhiqun, et al. Discrete wavelet transform for multiple decomposition of gravity anomalies. *Chinese journal of Geophysics*, 2001, 44(4):534–541. (in Chinese)
- [7] Zhu Silin, Gan Jiasi and Shen Chongyang. Three dimensional inversion of gravity anomalies in the western Yunnan. *Crustal Deformation and Earthquake*, 1994, 14(1):1–10. (in Chinese)
- [8] Chen Xuebo. Characteristics of deep structure of Three Gorges and adjacent area. Beijing: Earthquake Press, 1994. (in Chinese)
- [9] Yuan Dengwei and Mei Yingtang. Stability of crust of Three Gorges and adjacent area. Wuhan: China University of Geosciences Press, 1996, 17–40. (in Chinese)
- [10] Liao Wulin, Yao Yunsheng and Ding Zhifeng. Tomographic imagery of P wave velocity structure in Three Gorges region. *Journal of Geodesy and Geodynamics*, 2007, 27(3): 80–84. (in Chinese)
- [11] Zou Zhihui, Zhou Huawei and Liao Wulin. Crustal and upper-mantle seismic reflectors beneath the Three Gorges reservoir region. *Journal of Earth Science*, 2011, 22(2): 205–213. (in Chinese)
- [12] Gao Shijun, et al. Crust stress field and earthquake in Three Gorges region. Beijing: Seismological Press, 1992, 15–26. (in Chinese)
- [13] Han Xiaoguang, et al. A study on seismotectonic environment of the Zigui earthquake with $M = 5.1$ in western hubei province. *Journal of Seismological Research*, 1994, 17(1): 61–66. (in Chinese)